CRYSTALLOGRAPHIC COMMUNICATIONS

ISSN 2056-9890

Synthesis and structure of (*E*)-3,4,5-trihydroxy-*N*′-(3,4,5-trimethoxybenzylidene)benzohydrazide monohydrate

Mamadou Lo,[a]* Bineta Sene,[a] Adji Fatou Fall Pouye,[a] Arie van der Lee,[b] Abdoulaye Gassama[a] and Sébastien Richeter[c]

[a]Département de Chimie, UFR des Sciences et Technologies, Laboratoire de Chimie Physique des Matériaux (LCPM), BP 523, Ziguinchor, Senegal, [b]Institut Européen des Membranes, Université de Montpellier, CNRS, ENSCM, 34095 Montpellier, France, and [c]ICGM, Univ. Montpellier, CNRS, ENSCM, 34293 Montpellier, France. *Correspondence e-mail: mlo@univ-zig.sn

Received 7 April 2025
Accepted 5 May 2025

Edited by B. Therrien, University of Neuchâtel, Switzerland

Keywords: crystal structure; gallic acid; acylhydrazone.

CCDC reference: 2449013

Supporting information: this article has supporting information at journals.iucr.org/e

In the structure of the title compound, $C_{17}H_{18}N_2O_7{\cdot}H_2O$, hydrogen bonds link three molecules to the water molecule. Additional hydrogen-bonding interactions connect two molecules *via* the amide nitrogen donor and two methoxy oxygen acceptors. This three-dimensional hydrogen-bond network has no particular directionality, and a slight disorder of two methoxy groups is observed. According to force-field calculations, weaker but more extended van der Waals interactions show a larger stabilization effect than the hydrogen-bond interactions, while hydrogen-bond analysis suggests that polymorphs of the compound may be found in the future.

1. Introduction

Gallic acid is a secondary natural metabolite widely found in various fruits and vegetables (Zhou *et al.*, 2020; Hadidi *et al.*, 2024). Structurally, it is a low-molecular-weight phenolic acid, identified as 3,4,5-trihydroxybenzoic acid, and it is studied extensively for its remarkable antioxidant properties, which have applications in medicinal chemistry and various industrial sectors (Badhani *et al.*, 2015).

Acylhydrazones [*R*—C(=O)—NH—N=CH—*R*′] represent a class of organic compounds resulting from the combination of a hydrazone function and a carbonyl group. Synthetically, they are obtained through the condensation of a hydrazide, typically derived from a carboxylic acid or its ester, with an aldehyde or ketone (Oliveira *et al.*, 2022; Haranahalli *et al.*, 2019; Vlad *et al.*, 2024). This straightforward and efficient synthetic method accounts for its growing use in various fields of modern chemistry (Liu *et al.*, 2020). In materials chemistry, acylhydrazones are employed to develop promising materials such as reversible polymers (Ramimoghadam *et al.*, 2024) and tunable photoswitches (van Dijken *et al.*, 2015). Moreover, their structure exhibits keto–enol tautomeric equilibrium, which underlies their extensive use as multidentate ligands in coordination chemistry (Liu *et al.*, 2022). Additionally, the structural similarity between acylhydrazones and peptides explains their widespread application in medicinal chemistry. Numerous studies have shown that acylhydrazones exhibit a broad range of biological activities (Socea *et al.*, 2022; Kassab, 2023; Maia *et al.*, 2014).

In this context, acylhydrazones derived from gallic acid emerge as a particularly promising class of compounds, combining the antioxidant and metal-chelating properties of gallic acid with the versatile chemical behavior of acyl-

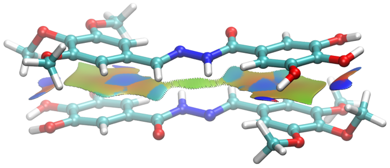

hydrazones. This simple and efficient methodology allows access to a wide range of gallic acid-based acylhydrazones with tunable properties. As part of our research efforts, we successfully characterized the crystallographic structure of the title compound (TTMB·H_2O), paving the way for further structural and biological investigations.

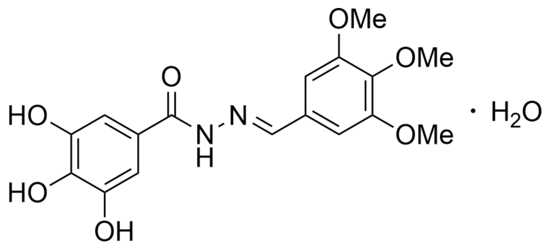

2. Structural commentary

All bond lengths and angles are comparable to those of similar fragments present in the Cambridge Structural Database: a default *Mogul* check (Bruno *et al.*, 2004) gave no unusual features. The molecular structure of the major disordered component of TTMB·H_2O is shown in Fig. 1. The gallic acid phenyl ring and the trimethoxy phenyl ring are inclined slightly with respect to each other, subtending a dihedral angle of 10.56 (2)°. The dihedral angle between the central acylhydrazone motif and the trimethoxy phenyl ring is 14.01 (2)°, whereas that with the gallic acid phenyl ring is 12.64 (3)°. The methoxy group in the 3-position is in a close to perpendicular orientation with respect to the ring to which it is attached [C7—O6—C5—C2 torsion angle = −86.57 (9)°], whereas the disordered methoxy groups in the 2 and 4 positions are not far from coplanarity with the ring. The occupancy factors of the methyl groups of the 2,4 methoxy moieties are 0.54 (2)/0.46 (2) and 0.39 (3)/0.61 (3), respectively. The presence of the water molecule in the crystal structure is probably due to traces of water in the ethanol used for the crystallization.

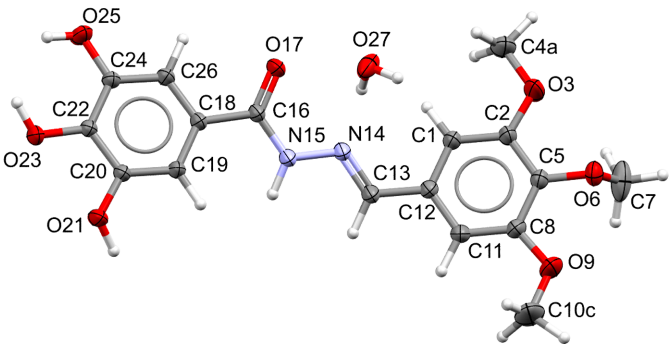

Figure 1
A view of the title structure showing the atom-labeling scheme. The atomic displacement ellipsoids are drawn at the 50% probability level. Only the major components of the disordered methoxy groups are shown. The isotropically refined hydrogen atoms have been drawn as fixed-sized spheres of 0.12 Å radius. The bond radius is 0.08 Å.

Table 1
Hydrogen-bond geometry (Å, °).

D—H···A	D—H	H···A	D···A	D—H···A
O23—H231···O27^{i}	0.941 (10)	1.748 (10)	2.6892 (7)	179.3 (9)
O21—H211···O17^{ii}	0.955 (11)	1.790 (11)	2.7246 (7)	165.3 (10)
O25—H251···O27^{i}	0.954 (11)	1.811 (11)	2.7649 (8)	177.5 (10)
N15—H151···O23^{iii}	0.985 (9)	2.115 (9)	3.0491 (7)	157.7 (8)
N15—H151···O21^{iii}	0.985 (9)	2.320 (9)	2.9572 (8)	121.6 (7)
O27—H271···O6^{iv}	0.938 (11)	1.858 (12)	2.7746 (8)	165.1 (10)
O27—H272···N14	0.973 (12)	1.956 (12)	2.8930 (8)	161.0 (10)

Symmetry codes: (i) $-x, -y, -z$; (ii) $x, -y + \frac{1}{2}, z - \frac{1}{2}$; (iii) $-x, y + \frac{1}{2}, -z - \frac{1}{2}$; (iv) $-x + 1, y - \frac{1}{2}, -z + \frac{1}{2}$.

3. Supramolecular features

The most prominent supramolecular feature in the structure of TTMB·H_2O is the water molecule that connects three TTMB moieties by short hydrogen bonds (Table 1, Fig. 2): donor–acceptor distances 2.8930 (8) (O27···N14), 2.7746 (8) (O27···O6), 2.7649 (8) (O25···O27), and 2.6892 Å (O23···O27). The latter two hydrogen bonds show a bifurcated bond involving two donor oxygen atoms of two neighboring hydroxyl groups of the same TTMB moiety, whereas the water oxygen acts as a single acceptor. An additional bifurcated hydrogen bond is found between two TTMB moieties, but involving the opposite configuration, *i.e.* two acceptor oxygen atoms and one donor nitrogen. The two acceptor oxygen atoms belong to two neighboring methoxy groups and connect to an amide nitrogen donor of a neighboring moiety. Such bifurcated hydrogen bonds are not rare and have been observed in α-helices, where it was shown that the interaction energy of bifurcated hydrogen bonds is in general 50 to 60% smaller than those of a canonical single donor–single acceptor hydrogen bond (Feldblum & Arkin, 2024). A hydrogen-bond coordination analysis (Galek *et al.*, 2014) shows that the likelihood of an acyclic amide nitrogen

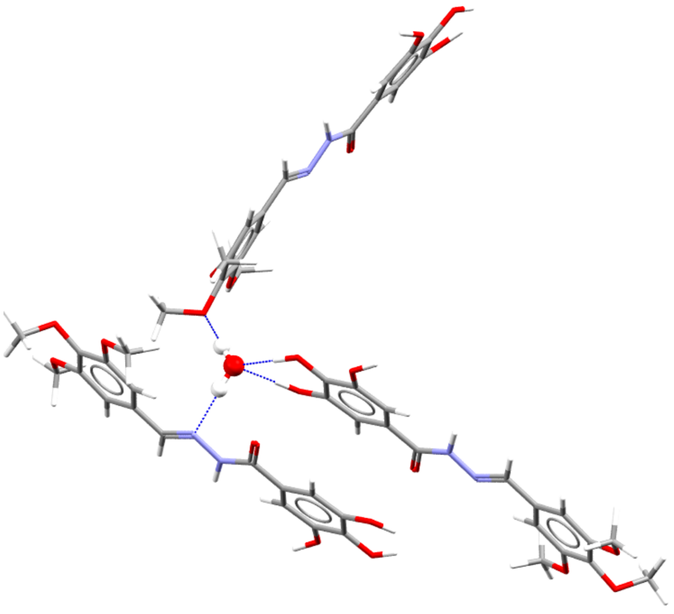

Figure 2
Hydrogen-bonded network between water and three TTMB moieties.

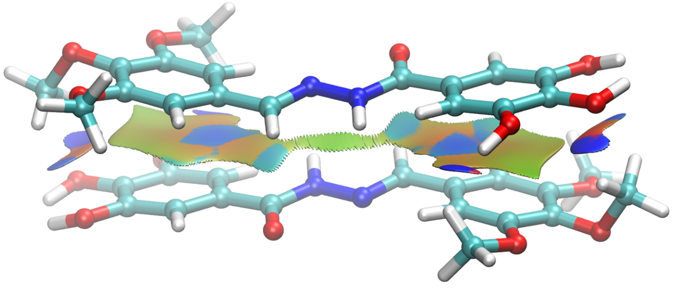

Figure 3

Non-covalent interaction regions between two nearly parallel TTMB moieties. The reduced electron density gradient [$s(\rho)$; see Johnson *et al.*, 2010] isosurface is drawn at the level of 0.3 atomic units and is color mapped based on the value of sin (λ)ρ: −0.1 (blue) < 0.0 (green) < 0.1 (red), where ρ is the electron density and λ the second electron density Hessian eigenvalue.

donor (N15) having a bifurcated hydrogen bond is very low (2.4%), compared to that of a – not observed – single hydrogen bond (86%). The probability of water oxygen atoms accepting two donors – as is observed in this structure – remains relatively low (29%) compared to the acceptance of only one donor (65%). Two of the three acceptor oxygen atoms of the methoxy groups show no intermolecular interactions. The overall hydrogen-bond coordination capacity in TTMB·H_20 is only fulfilled at 56%, leaving the possibility open that one or more polymorphs may exist.

A full hydrogen-bond statistical analysis shows that the water oxygen (O27) to amide nitrogen distance (N14) 2.8930 (8) Å, is unusually short, falling within the lower 5% quantile for 591 analogs. The same is true for the O27···O6 donor–acceptor pair distance [2.7746 (8) Å; 746 observations]. The N15—H151···O21 angle [121.6 (7)°] is also found to be unusually small, whereas the N15—H151···O23 angle falls within the expected range. This bifurcated hydrogen bond appears to be constituted of a strong and weak component.

The hydrogen-bond network has no particular directionality and can thus be considered as three-dimensional. Although the hydrogen-bond network alone might seem essential for the stabilization of the structural architecture, there may be other interactions that play a role. There are no appreciable π–π interactions with centroid–centroid distances below 4.0 Å, and only one short C—H-centroid interaction, C7—H73···*Cg*2(C12–C1–C2–C5–C8–C11), 2.608 (6) Å. The interaction energies of different synthons that may contribute to the total lattice energy were calculated using the Momany force field, also called the CHARMm force field (Momany & Rone, 1992). In this force field, the interaction energy of each synthon is decomposed in three different terms: an electrostatic, a hydrogen bond, and a van der Waals energy term. The most important individual synthon links two parallel TTMB molecules with a slipped-parallel π–π stacking arrangement (Fig. 3). The energy decomposition shows that van der Waals interactions make up most of the total interaction energy, which is confirmed by a pictorial representation of the interaction zones calculated by the NCI index method (Fig. 3, Johnson *et al.*, 2010). The second most important synthon has two TTMB molecules in a nearly perpendicular orientation for which the hydrogen-bond interactions are 40% more important than the van der Waals interactions. The synthons that link the water molecule to the neighboring TTMB molecules have the most important energy contribution, while the van der Waals energy is negligible. From the decomposition of the total lattice energy, it appears that – according to the Momany force field – approximately 46% of the stabilization is accounted for by van der Waals-type interactions, 31% by hydrogen-bond interactions and 23% by electrostatic interactions.

4. Database survey

A search of the Cambridge Structural Database (version 5.46 with November 2024 updates; Groom *et al.*, 2016) revealed 14 entries for gallic acid acylhydrazone derivatives, of which one contains a metal center (IDUVEK; Alhadi *et al.*, 2012). The hydroxynaphthalene derivative (LUYHUL; Shaikh *et al.*, 2020) was reported to be used as a nano-molar detection probe for the catalytic activity of La^{3+} ions *in vivo*. The structure that is most closely related to the title compound is the 2,4-dimethoxyphenyl derivative (SOYCON; Alhadi *et al.*, 2009) but instead of a water solvate, it is an ethanol solvate. Among the fourteen related structures seven are water solvates, two are methanol solvates and one is an ethanol solvate, while the others have no solvent of crystallization.

5. Synthesis and crystallization

The title compound was synthesized in a round-bottom flask by dissolving 3,4,5-trihydroxybenzohydrazide (1.1 mmol, 0.2 g) in absolute ethanol (2 mL). Subsequently, a solution of 3,4,5-trimethoxybenzaldehyde (1.0 mmol, 0.196 g) in absolute ethanol (2 mL) was added dropwise under continuous stirring, followed by the addition of a single drop of acetic acid as a catalyst. The reaction mixture was refluxed for approximately 3 h, leading to the formation of a white precipitate. The resulting solid was collected by filtration, washed thoroughly with cold ethanol, and air-dried. Single crystals suitable for X-ray diffraction analysis were obtained by slow evaporation of an ethanol solution of the title compound at room temperature over several days. Standard characterization data for TTMB are available in the literature (Peng *et al.*, 2022).

6. Refinement

Crystal data, data collection and structure refinement details are summarized in Table 2. An initial structure refinement was carried out using *OLEX2* (Dolomanov *et al.*, 2009) using spherical scattering factors for all atoms. The methyl groups of the two methoxy groups in the 2- and 4-positions were found to be slightly disordered over two different positions. The relative occupancies were refined while keeping the sum at 1.0 with soft restraints set on the oxygen-to-carbon distances, and similarity restraints on the atomic displacement parameters of each disordered group. The difference-Fourier map showed residual densities in the centers of almost all covalent bonds,

Acta Cryst. (2025). E**81** Lo *et al.* • $C_{17}H_{18}N_2O_7{\cdot}H_2O$ **3 of 4**

Table 2
Experimental details.

Crystal data	
Chemical formula	$C_{17}H_{18}N_2O_7{\cdot}H_2O$
M_r	380.36
Crystal system, space group	Monoclinic, $P2_1/c$
Temperature (K)	173
a, b, c (Å)	11.5409 (7), 10.9018 (6), 14.3799 (8)
β (°)	103.427 (2)
V (Å^3)	1759.78 (17)
Z	4
Radiation type	Mo $K\alpha$
μ (mm^{-1})	0.12
Crystal size (mm)	0.34 × 0.23 × 0.04
Data collection	
Diffractometer	Venture Photon-II
Absorption correction	Multi-scan (*SADABS*; Krause *et al.*, 2015)
$T_{\min}$, $T_{\max}$	0.95, 1.00
No. of measured, independent and observed [$I \geq 2u(I)$] reflections	57780, 7401, 5802
$R_{\rm int}$	0.059
$(\sin \theta/\lambda)_{\max}$ (Å^{-1})	0.796
Refinement	
$R[F^2 > 2\sigma(F^2)]$, $wR(F^2)$, S	0.035, 0.062, 1.08
No. of reflections	7401
No. of parameters	342
No. of restraints	16
H-atom treatment	Only H-atom coordinates refined
$\Delta\rho_{\max}$, $\Delta\rho_{\min}$ (e Å^{-3})	0.30, −0.30

Computer programs: *SUPERFLIP* (Palatinus & Chapuis, 2007), *OLEX2.refine* (Bourhis *et al.*, 2015), *Mercury* (Macrae *et al.*, 2020; *VMD* (Humphrey *et al.*, 1996) and *OLEX2* (Dolomanov *et al.*, 2009).

so it was decided to perform the final refinement according to the Hirshfeld Atom Refinement (HAR) methodology using aspherical scattering factors as implemented in the *OLEX2* software package. The electron density was calculated from a Gaussian basis set single determinant SCF wave function (DFT-r2SCAN, cc-pVTZ basis set) with the *ORCA 6.0* package (Neese, 2012) and partitioning according to the NoSpherA2 methodology (Kleemiss *et al.*, 2021). The positions and isotropic atomic displacement parameters of the hydrogen atoms were freely refined. The four disordered parts were treated for the calculation of the wavefunctions according to the grouped parts method, giving four different structures (syntax 1-2;3,4 for parts 1/3, 1/4, 2/3, 2/4), recently described by Kleemiss *et al.* (2021).

Acknowledgements

The authors are grateful to the French Embassy in Senegal for funding the three-month research stay at the Charles Gerhardt Institute in Montpellier. We also extend our sincere thanks to Ms Dominique Granier for her valuable technical assistance in the measurement of the X-ray diffraction data.

References

Alhadi, A. A., Saharin, S. M., Mohd Ali, H., Robinson, W. T. & Abdulla, M. A. (2009). *Acta Cryst.* E**65**, o1373.

Alhadi, A. A., Shaker, S. A., Suleiman, N., Yehye, W. A. & Mohd Ali, H. (2012). *J. Chil. Chem. Soc.* **57**, 1283–1286.

Badhani, B., Sharma, N. & Kakkar, R. (2015). *RSC Adv.* **5**, 27540–27557.

Bourhis, L. J., Dolomanov, O. V., Gildea, R. J., Howard, J. A. K. & Puschmann, H. (2015). *Acta Cryst.* A**71**, 59–75.

Bruno, I. J., Cole, J. C., Kessler, M., Luo, J., Motherwell, W. D. S., Purkis, L. H., Smith, B. R., Taylor, R., Cooper, R. I., Harris, S. E. & Orpen, A. G. (2004). *J. Chem. Inf. Comput. Sci.* **44**, 2133–2144.

Dolomanov, O. V., Bourhis, L. J., Gildea, R. J., Howard, J. A. K. & Puschmann, H. (2009). *J. Appl. Cryst.* **42**, 339–341.

Feldblum, E. S. & Arkin, I. (2024). *Proc. Natl. Acad. Sci.* **111**, 4085–4090.

Galek, P. T. A., Chisholm, J. A., Pidcock, E. & Wood, P. A. (2014). *Acta Cryst.* B**70**, 91–105.

Groom, C. R., Bruno, I. J., Lightfoot, M. P. & Ward, S. C. (2016). *Acta Cryst.* B**72**, 171–179.

Hadidi, M., Liñán-Atero, R., Tarahi, M., Christodoulou, M. C. & Aghababaei, F. (2024). *Antioxidants*, **13**, 1001.

Haranahalli, K., Lazzarini, C., Sun, Y., Zambito, J., Pathiranage, S., McCarthy, J. B., Mallamo, J., Del Poeta, M. & Ojima, I. (2019). *J. Med. Chem.* **62**, 8249–8273.

Humphrey, W., Dalke, A. & Schulten, K. (1996). *J. Mol. Graph.* **14**, 1996, 33–38.

Johnson, E. R., Keinan, S., Mori-Sánchez, P., Contreras-García, J., Cohen, A. J. & Yang, W. (2010). *J. Am. Chem. Soc.* **132**, 6498–6506.

Kassab, A. E. (2023). *Arch. Pharm.* **356**, 2200548.

Kleemiss, F., Dolomanov, O. V., Bodensteiner, M., Peyerimhoff, N., Midgley, L., Bourhis, L. J., Genoni, A., Malaspina, L. A., Jayatilaka, D., Spencer, J. L., White, F., Grundkötter-Stock, B., Steinhauer, S., Lentz, D., Puschmann, H. & Grabowsky, S. (2021). *Chem. Sci.* **12**, 1675–1692.

Krause, L., Herbst-Irmer, R., Sheldrick, G. M. & Stalke, D. (2015). *J. Appl. Cryst.* **48**, 3–10.

Liu, R., Cui, J., Ding, T., Liu, Y. & Liang, H. (2022). *Molecules* **27**, 8393.

Liu, Y., Peng, Q., Li, Y., Hou, H. & Li, K. (2020). *Chin. Chem. Lett.* **31**, 3271–3275.

Macrae, C. F., Sovago, I., Cottrell, S. J., Galek, P. T. A., McCabe, P., Pidcock, E., Platings, M., Shields, G. P., Stevens, J. S., Towler, M. & Wood, P. A. (2020). *J. Appl. Cryst.* **53**, 226–235.

Maia, R., Tesch, R. & Fraga, C. A. M. (2014). *Expert Opin. Ther. Pat.* **24**, 1161–1170.

Momany, F. A. & Rone, R. (1992). *J. Comput. Chem.* **13**, 888–900.

Neese, F. (2012). *WIREs Comput. Mol. Sci.* **2**, 73–78.

Oliveira, F. A., Pinto, A. C. S., Duarte, C. L., Taranto, A. G., Lorenzato Junior, E., Cordeiro, C. F., Carvalho, D. T., Varotti, F. P. & Fonseca, A. L. (2022). *BMC Chem.* **16**, 50.

Palatinus, L. & Chapuis, G. (2007). *J. Appl. Cryst.* **40**, 786–790.

Peng, Z., Li, Y., Tan, L., Chen, L., Shi, Q., Zeng, Q.-H., Liu, H., Wang, J. J. & Zhao, Y. (2022). *Food Chem.* **378**, 132127.

Ramimoghadam, D., Eyckens, D. J., Evans, R. A., Moad, G., Holmes, S. & Simons, R. (2024). *Chem. A Eur. J.* **30**, e202401728.

Shaikh, A., Ghosh, M., Mukherjee, P., Ghosh, A., Molla, R. A., Ta, S. & Das, D. (2020). *New J. Chem.* **44**, 13501–13506.

Socea, L.-I., Barbuceanu, S.-F., Pahontu, E. M., Dumitru, A.-C., Nitulescu, G. M., Sfetea, R. C. & Apostol, T.-V. (2022). *Molecules*, **27**, 8719.

van Dijken, D. J., Kovaříček, P., Ihrig, S. P. & Hecht, S. (2015). *J. Am. Chem. Soc.* **137**, 14982–14991.

Vlad, I. M., Nuţă, D. C., Căproiu, M. T., Dumitraşcu, F., Kapronczai, E., Mük, G. R., Avram, S., Niculescu, A. G., Zarafu, I., Ciorobescu, V. A., Brezeanu, A. M. & Limban, C. (2024). *Antibiotics*, **13**, 212.

Zhou, X., Zeng, L., Chen, Y., Wang, X., Liao, Y., Xiao, Y., Fu, X. & Yang, Z. (2020). *Int. J. Mol. Sci.* **21**, 5684.

supporting information

Acta Cryst. (2025). E**81** [https://doi.org/10.1107/S2056989025004001]

Synthesis and structure of (*E*)-3,4,5-trihydroxy-*N′*-(3,4,5-trimethoxybenzylidene)benzohydrazide monohydrate

Mamadou Lo, Bineta Sene, Adji Fatou Fall Pouye, Arie van der Lee, Abdoulaye Gassama and Sébastien Richeter

Computing details

(*E*)-3,4,5-Trihydroxy-*N′*-(3,4,5-trimethoxybenzylidene)benzohydrazide monohydrate

Crystal data

$C_{17}H_{18}N_2O_7 \cdot H_2O$
$M_r = 380.36$
Monoclinic, $P2_1/c$
$a = 11.5409\ (7)$ Å
$b = 10.9018\ (6)$ Å
$c = 14.3799\ (8)$ Å
$\beta = 103.427\ (2)$°
$V = 1759.78\ (17)$ Å^3
$Z = 4$
$F(000) = 800.657$
$D_x = 1.436$ Mg m^{-3}
Mo $K\alpha$ radiation, $\lambda = 0.71073$ Å
Cell parameters from 9902 reflections
$\theta = 2.4$–34.3°
$\mu = 0.12$ mm^{-1}
$T = 173$ K
Prism, colourless
0.34 × 0.23 × 0.04 mm

Data collection

Venture Photon-II
diffractometer
φ and ω scans
Absorption correction: multi-scan
(SADABS; Krause *et al.*, 2015)
$T_{min} = 0.95$, $T_{max} = 1.00$
57780 measured reflections
7401 independent reflections
5802 reflections with $I \geq 2u(I)$
$R_{int} = 0.059$
$\theta_{max} = 34.5°$, $\theta_{min} = 2.4°$
$h = -18 \rightarrow 18$
$k = -17 \rightarrow 17$
$l = -22 \rightarrow 22$

Refinement

Refinement on F^2
Least-squares matrix: full
$R[F^2 > 2\sigma(F^2)] = 0.035$
$wR(F^2) = 0.062$
$S = 1.08$
7401 reflections
342 parameters
16 restraints
28 constraints
Primary atom site location: iterative
Hydrogen site location: difference Fourier map
Only H-atom coordinates refined
$w = 1/[\sigma^2(F_o^2) + (0.0094P)^2 + 0.2877P]$
where $P = (F_o^2 + 2F_c^2)/3$
$(\Delta/\sigma)_{max} = 0.001$
$\Delta\rho_{max} = 0.30$ e Å^{-3}
$\Delta\rho_{min} = -0.29$ e Å^{-3}

Fractional atomic coordinates and isotropic or equivalent isotropic displacement parameters (Å^2)

	x	y	z	U_{iso}*/U_{eq}	Occ. (<1)
O23	−0.16740 (5)	−0.10296 (4)	−0.27135 (3)	0.01723 (10)	

H231	−0.2026 (9)	−0.1681 (9)	−0.2449 (7)	0.02584 (14)*	
O21	−0.00615 (5)	0.04187 (5)	−0.31462 (3)	0.02050 (11)	
H211	0.0150 (10)	0.1127 (10)	−0.3460 (7)	0.03076 (16)*	
O17	0.01977 (5)	0.26329 (5)	0.07329 (3)	0.01894 (10)	
O3	0.31182 (6)	0.71678 (6)	0.31595 (4)	0.03290 (15)	
O6	0.49176 (4)	0.83971 (5)	0.27220 (4)	0.01874 (10)	
O9	0.53534 (5)	0.82814 (6)	0.09931 (4)	0.03169 (14)	
O25	−0.23283 (5)	−0.07336 (5)	−0.09043 (4)	0.02225 (11)	
H251	−0.2469 (10)	−0.1477 (10)	−0.1263 (8)	0.03337 (17)*	
N15	0.10103 (5)	0.35562 (5)	−0.03782 (4)	0.01652 (11)	
H151	0.0992 (8)	0.3707 (8)	−0.1057 (6)	0.01982 (13)*	
N14	0.16027 (5)	0.43628 (5)	0.02928 (4)	0.01534 (10)	
C22	−0.11988 (6)	−0.01524 (6)	−0.20606 (4)	0.01278 (11)	
C20	−0.03649 (6)	0.06508 (6)	−0.23039 (4)	0.01397 (11)	
C19	0.01409 (6)	0.15878 (6)	−0.16865 (5)	0.01610 (12)	
H191	0.0802 (7)	0.2141 (8)	−0.1889 (6)	0.01932 (14)*	
C18	−0.01895 (6)	0.17342 (6)	−0.08161 (4)	0.01353 (11)	
C16	0.03388 (6)	0.26711 (6)	−0.00924 (4)	0.01391 (11)	
C13	0.21854 (6)	0.52293 (6)	0.00037 (5)	0.01643 (12)	
H131	0.2215 (7)	0.5313 (7)	−0.0733 (6)	0.01972 (14)*	
C12	0.28525 (6)	0.61051 (6)	0.06973 (4)	0.01459 (11)	
C1	0.25992 (6)	0.62084 (6)	0.15975 (5)	0.01662 (12)	
H11	0.1882 (7)	0.5690 (8)	0.1756 (6)	0.01994 (15)*	
C2	0.32763 (6)	0.69985 (6)	0.22673 (5)	0.01729 (12)	
C5	0.42032 (6)	0.76765 (6)	0.20393 (5)	0.01525 (12)	
C7	0.44587 (8)	0.96035 (8)	0.27896 (8)	0.0344 (2)	
H71	0.4434 (10)	1.0070 (10)	0.2129 (8)	0.0517 (3)*	
H72	0.3597 (10)	0.9547 (10)	0.2945 (8)	0.0517 (3)*	
H73	0.5075 (10)	1.0059 (10)	0.3340 (8)	0.0517 (3)*	
C8	0.44380 (6)	0.75848 (6)	0.11305 (5)	0.01781 (13)	
C11	0.37541 (6)	0.67979 (6)	0.04516 (5)	0.01825 (13)	
H111	0.3905 (7)	0.6718 (8)	−0.0256 (6)	0.02190 (15)*	
C26	−0.10082 (6)	0.09328 (6)	−0.05723 (5)	0.01540 (12)	
H261	−0.1239 (7)	0.1025 (8)	0.0107 (6)	0.01848 (14)*	
C24	−0.15188 (6)	−0.00032 (6)	−0.11857 (5)	0.01416 (11)	
O27	0.26649 (5)	0.28900 (5)	0.19444 (4)	0.02384 (11)	
H271	0.3461 (10)	0.3139 (10)	0.2147 (8)	0.03577 (17)*	
H272	0.2198 (10)	0.3454 (11)	0.1480 (9)	0.03577 (17)*	
C4a	0.2110 (5)	0.6593 (5)	0.3378 (3)	0.0297 (8)	0.54 (2)
H4a1	0.126 (2)	0.672 (2)	0.2865 (16)	0.0446 (13)*	0.54 (2)
H4a2	0.223 (3)	0.559 (3)	0.3363 (18)	0.0446 (13)*	0.54 (2)
H4a3	0.2086 (19)	0.693 (2)	0.4071 (15)	0.0446 (13)*	0.54 (2)
C4b	0.2449 (9)	0.6202 (11)	0.3523 (4)	0.0425 (19)	0.46 (2)
H4b1	0.153 (3)	0.639 (4)	0.320 (3)	0.064 (3)*	0.46 (2)
H4b2	0.272 (3)	0.527 (3)	0.342 (2)	0.064 (3)*	0.46 (2)
H4b3	0.263 (3)	0.626 (3)	0.428 (2)	0.064 (3)*	0.46 (2)
C10d	0.5545 (17)	0.8358 (16)	0.0054 (8)	0.049 (3)	0.39 (3)
H10d1	0.564 (5)	0.751 (5)	−0.028 (4)	0.074 (4)*	0.39 (3)

H10d2	0.477 (4)	0.869 (4)	−0.046 (3)	0.074 (4)*	0.39 (3)
H10d3	0.616 (4)	0.909 (4)	0.006 (3)	0.074 (4)*	0.39 (3)
C10c	0.5817 (7)	0.8001 (10)	0.0173 (6)	0.0452 (14)	0.61 (3)
H10c1	0.606 (2)	0.707 (2)	0.015 (2)	0.068 (2)*	0.61 (3)
H10c2	0.511 (3)	0.823 (3)	−0.050 (2)	0.068 (2)*	0.61 (3)
H10c3	0.660 (2)	0.857 (3)	0.0249 (17)	0.068 (2)*	0.61 (3)

Atomic displacement parameters (Å^2)

	U^{11}	U^{22}	U^{33}	U^{12}	U^{13}	U^{23}
O23	0.0230 (2)	0.0151 (2)	0.0147 (2)	−0.00580 (18)	0.00659 (19)	−0.00383 (17)
O21	0.0317 (3)	0.0189 (2)	0.0142 (2)	−0.0083 (2)	0.0119 (2)	−0.00423 (18)
O17	0.0275 (3)	0.0186 (2)	0.0125 (2)	−0.0064 (2)	0.00826 (19)	−0.00412 (18)
O3	0.0381 (3)	0.0441 (4)	0.0216 (3)	−0.0233 (3)	0.0174 (3)	−0.0159 (3)
O6	0.0155 (2)	0.0193 (2)	0.0202 (2)	−0.00291 (18)	0.00158 (18)	−0.00466 (19)
O9	0.0320 (3)	0.0398 (3)	0.0267 (3)	−0.0219 (3)	0.0137 (2)	−0.0063 (3)
O25	0.0248 (3)	0.0230 (3)	0.0232 (3)	−0.0101 (2)	0.0143 (2)	−0.0044 (2)
N15	0.0242 (3)	0.0144 (2)	0.0106 (2)	−0.0058 (2)	0.0032 (2)	−0.00096 (19)
N14	0.0210 (3)	0.0133 (2)	0.0111 (2)	−0.0041 (2)	0.0024 (2)	−0.00061 (19)
C22	0.0155 (3)	0.0123 (3)	0.0113 (3)	−0.0021 (2)	0.0047 (2)	−0.0009 (2)
C20	0.0185 (3)	0.0133 (3)	0.0113 (3)	−0.0037 (2)	0.0058 (2)	−0.0017 (2)
C19	0.0212 (3)	0.0159 (3)	0.0130 (3)	−0.0069 (2)	0.0077 (2)	−0.0030 (2)
C18	0.0170 (3)	0.0131 (3)	0.0112 (3)	−0.0028 (2)	0.0047 (2)	−0.0023 (2)
C16	0.0183 (3)	0.0131 (3)	0.0106 (3)	−0.0024 (2)	0.0039 (2)	−0.0017 (2)
C13	0.0218 (3)	0.0150 (3)	0.0119 (3)	−0.0044 (2)	0.0027 (2)	−0.0005 (2)
C12	0.0174 (3)	0.0137 (3)	0.0125 (3)	−0.0032 (2)	0.0030 (2)	0.0001 (2)
C1	0.0182 (3)	0.0173 (3)	0.0153 (3)	−0.0059 (2)	0.0060 (2)	−0.0030 (2)
C2	0.0189 (3)	0.0195 (3)	0.0146 (3)	−0.0064 (2)	0.0063 (2)	−0.0047 (2)
C5	0.0149 (3)	0.0153 (3)	0.0155 (3)	−0.0030 (2)	0.0033 (2)	−0.0019 (2)
C7	0.0271 (4)	0.0226 (4)	0.0480 (6)	−0.0002 (3)	−0.0028 (4)	−0.0147 (4)
C8	0.0184 (3)	0.0196 (3)	0.0160 (3)	−0.0067 (2)	0.0052 (2)	−0.0003 (2)
C11	0.0223 (3)	0.0198 (3)	0.0131 (3)	−0.0071 (2)	0.0052 (2)	−0.0002 (2)
C26	0.0188 (3)	0.0159 (3)	0.0135 (3)	−0.0038 (2)	0.0079 (2)	−0.0036 (2)
C24	0.0159 (3)	0.0145 (3)	0.0136 (3)	−0.0033 (2)	0.0066 (2)	−0.0021 (2)
O27	0.0203 (2)	0.0206 (3)	0.0272 (3)	−0.0067 (2)	−0.0013 (2)	0.0062 (2)
C4a	0.0357 (17)	0.0344 (16)	0.0244 (12)	−0.0135 (12)	0.0179 (12)	−0.0065 (10)
C4b	0.050 (3)	0.060 (4)	0.0238 (15)	−0.032 (3)	0.0208 (17)	−0.0121 (19)
C10d	0.059 (6)	0.060 (5)	0.036 (3)	−0.038 (4)	0.028 (4)	−0.011 (3)
C10c	0.043 (2)	0.065 (4)	0.0345 (16)	−0.0290 (19)	0.0243 (15)	−0.0085 (18)

Geometric parameters (Å, º)

O23—H231	0.940 (10)	C12—C1	1.3962 (9)
O23—C22	1.3629 (8)	C12—C11	1.3960 (9)
O21—H211	0.955 (11)	C1—H11	1.070 (8)
O21—C20	1.3603 (8)	C1—C2	1.3894 (9)
O17—C16	1.2356 (8)	C2—C5	1.4004 (9)
O3—C2	1.3499 (8)	C5—C8	1.3985 (9)

O3—C4a	1.420 (3)	C7—H71	1.072 (11)
O3—C4b	1.471 (6)	C7—H72	1.070 (11)
O6—C5	1.3729 (8)	C7—H73	1.057 (11)
O6—C7	1.4295 (10)	C8—C11	1.3979 (9)
O9—C8	1.3523 (8)	C11—H111	1.075 (8)
O9—C10d	1.421 (9)	C26—H261	1.075 (8)
O9—C10c	1.436 (6)	C26—C24	1.3875 (9)
O25—H251	0.954 (11)	O27—H271	0.937 (11)
O25—C24	1.3587 (8)	O27—H272	0.973 (12)
N15—H151	0.985 (9)	C4a—H4a1	1.09 (2)
N15—N14	1.3656 (7)	C4a—H4a2	1.10 (3)
N15—C16	1.3596 (8)	C4a—H4a3	1.07 (2)
N14—C13	1.2835 (8)	C4b—H4b1	1.07 (3)
C22—C20	1.4041 (9)	C4b—H4b2	1.09 (3)
C22—C24	1.4006 (9)	C4b—H4b3	1.07 (3)
C20—C19	1.3899 (9)	C10d—H10d1	1.06 (5)
C19—H191	1.065 (8)	C10d—H10d2	1.09 (4)
C19—C18	1.3996 (9)	C10d—H10d3	1.07 (4)
C18—C16	1.4844 (9)	C10c—H10c1	1.05 (2)
C18—C26	1.3903 (9)	C10c—H10c2	1.14 (3)
C13—H131	1.071 (8)	C10c—H10c3	1.08 (3)
C13—C12	1.4637 (9)		

C22—O23—H231	113.2 (6)	H71—C7—O6	108.0 (6)
C20—O21—H211	114.7 (6)	H72—C7—O6	109.8 (6)
C4a—O3—C2	116.66 (17)	H72—C7—H71	112.2 (8)
C4b—O3—C2	115.9 (2)	H73—C7—O6	106.7 (6)
C4b—O3—C4a	23.2 (3)	H73—C7—H71	108.3 (8)
C7—O6—C5	113.86 (6)	H73—C7—H72	111.5 (8)
C10d—O9—C8	118.1 (5)	C5—C8—O9	115.08 (6)
C10c—O9—C8	116.9 (3)	C11—C8—O9	125.18 (6)
C10c—O9—C10d	20.3 (6)	C11—C8—C5	119.74 (6)
C24—O25—H251	112.3 (6)	C8—C11—C12	119.24 (6)
N14—N15—H151	119.0 (5)	H111—C11—C12	119.3 (4)
C16—N15—H151	122.4 (5)	H111—C11—C8	121.4 (4)
C16—N15—N14	118.06 (5)	H261—C26—C18	119.8 (4)
C13—N14—N15	117.33 (5)	C24—C26—C18	121.00 (6)
C20—C22—O23	117.09 (5)	C24—C26—H261	119.2 (4)
C24—C22—O23	123.53 (6)	C22—C24—O25	122.85 (6)
C24—C22—C20	119.36 (6)	C26—C24—O25	117.49 (6)
C22—C20—O21	116.03 (5)	C26—C24—C22	119.66 (6)
C19—C20—O21	123.28 (6)	H272—O27—H271	112.1 (9)
C19—C20—C22	120.64 (6)	H4a1—C4a—O3	116.6 (12)
H191—C19—C20	117.5 (4)	H4a2—C4a—O3	108.7 (13)
C18—C19—C20	119.59 (6)	H4a2—C4a—H4a1	102 (2)
C18—C19—H191	122.8 (4)	H4a3—C4a—O3	104.8 (11)
C16—C18—C19	123.54 (6)	H4a3—C4a—H4a1	111.8 (17)
C26—C18—C19	119.74 (6)	H4a3—C4a—H4a2	112.8 (18)

C26—C18—C16	116.63 (5)	H4b1—C4b—O3	105 (2)
N15—C16—O17	121.72 (6)	H4b2—C4b—O3	115.9 (17)
C18—C16—O17	121.73 (6)	H4b2—C4b—H4b1	114 (3)
C18—C16—N15	116.53 (5)	H4b3—C4b—O3	109.0 (15)
H131—C13—N14	121.5 (4)	H4b3—C4b—H4b1	112 (2)
C12—C13—N14	119.45 (6)	H4b3—C4b—H4b2	101 (2)
C12—C13—H131	119.1 (4)	H10d1—C10d—O9	116 (3)
C1—C12—C13	119.61 (6)	H10d2—C10d—O9	112 (2)
C11—C12—C13	119.04 (6)	H10d2—C10d—H10d1	98 (4)
C11—C12—C1	121.32 (6)	H10d3—C10d—O9	107 (2)
H11—C1—C12	119.6 (4)	H10d3—C10d—H10d1	121 (3)
C2—C1—C12	119.18 (6)	H10d3—C10d—H10d2	101 (3)
C2—C1—H11	121.2 (4)	H10c1—C10c—O9	112.6 (13)
C1—C2—O3	124.42 (6)	H10c2—C10c—O9	108.9 (16)
C5—C2—O3	115.43 (6)	H10c2—C10c—H10c1	109 (2)
C5—C2—C1	120.15 (6)	H10c3—C10c—O9	105.0 (13)
C2—C5—O6	119.95 (6)	H10c3—C10c—H10c1	109.4 (18)
C8—C5—O6	119.65 (6)	H10c3—C10c—H10c2	112.3 (19)
C8—C5—C2	120.35 (6)		

O23—C22—C20—O21	−3.99 (7)	O25—C24—C26—C18	−178.76 (6)
O23—C22—C20—C19	178.55 (6)	N15—N14—C13—C12	−178.94 (6)
O23—C22—C24—O25	0.70 (8)	N15—C16—C18—C19	12.19 (7)
O23—C22—C24—C26	−178.59 (6)	N15—C16—C18—C26	−171.26 (6)
O21—C20—C22—C24	177.39 (6)	N14—C13—C12—C1	−17.48 (8)
O21—C20—C19—C18	−177.57 (7)	N14—C13—C12—C11	160.80 (7)
O17—C16—N15—N14	4.59 (8)	C22—C20—C19—C18	−0.30 (8)
O17—C16—C18—C19	−166.24 (7)	C22—C24—C26—C18	0.57 (8)
O17—C16—C18—C26	10.31 (8)	C20—C19—C18—C16	177.24 (6)
O3—C2—C1—C12	−179.60 (7)	C20—C19—C18—C26	0.80 (8)
O3—C2—C5—O6	3.49 (8)	C19—C18—C26—C24	−0.94 (8)
O3—C2—C5—C8	−179.20 (6)	C13—C12—C1—C2	176.87 (6)
O6—C5—C2—C1	−175.92 (6)	C13—C12—C11—C8	−176.43 (6)
O6—C5—C8—O9	−2.67 (7)	C12—C1—C2—C5	−0.25 (8)
O6—C5—C8—C11	176.38 (6)	C12—C11—C8—C5	−0.65 (8)
O9—C8—C5—C2	−179.99 (6)	C1—C2—C5—C8	1.40 (8)
O9—C8—C11—C12	178.30 (7)	C2—C5—C8—C11	−0.94 (8)
O25—C24—C22—C20	179.23 (6)		

Hydrogen-bond geometry (Å, º)

D—H···*A*	*D*—H	H···*A*	*D*···*A*	*D*—H···*A*
O23—H231···O27$^{\text{i}}$	0.941 (10)	1.748 (10)	2.6892 (7)	179.3 (9)
O21—H211···O17$^{\text{ii}}$	0.955 (11)	1.790 (11)	2.7246 (7)	165.3 (10)
O25—H251···O27$^{\text{i}}$	0.954 (11)	1.811 (11)	2.7649 (8)	177.5 (10)
N15—H151···O23$^{\text{iii}}$	0.985 (9)	2.115 (9)	3.0491 (7)	157.7 (8)
N15—H151···O21$^{\text{iii}}$	0.985 (9)	2.320 (9)	2.9572 (8)	121.6 (7)
C19—H191···O23$^{\text{iii}}$	1.065 (8)	2.363 (8)	3.3661 (8)	156.4 (6)

C11—H111···O3^{iv}	1.076 (8)	2.555 (9)	3.3986 (9)	134.7 (6)
O27—H271···O6^{v}	0.938 (11)	1.858 (12)	2.7746 (8)	165.1 (10)
O27—H272···N14	0.973 (12)	1.956 (12)	2.8930 (8)	161.0 (10)
C10*d*—H10*d*2···O3^{iv}	1.09 (4)	2.59 (5)	3.472 (16)	138 (3)
C10*d*—H10*d*3···O25^{vi}	1.07 (4)	2.47 (4)	3.236 (11)	128 (3)
C10*c*—H10*c*3···O25^{vi}	1.08 (3)	2.41 (2)	3.229 (7)	131.4 (17)

Symmetry codes: (i) $-x, -y, -z$; (ii) $x, -y+1/2, z-1/2$; (iii) $-x, y+1/2, -z-1/2$; (iv) $x, -y+3/2, z-1/2$; (v) $-x+1, y-1/2, -z+1/2$; (vi) $x+1, y+1, z$.